nature microbiology

SUPPLEMENTARY INFORMATION

ARTICLE NUMBER: 16196 | DOI: 10.1038/NMICROBIOL.2016.196

A mucosal imprint left by prior *Escherichia coli* bladder infection sensitizes to recurrent disease

Valerie P. O'Brien[1], Thomas J. Hannan[1,2], Lu Yu[1], Jonathan Livny[3], Elisha D.O. Roberson[4,5], Drew J. Schwartz[1], Spenser Souza[6], Cathy L. Mendelsohn[6], Marco Colonna[2], Amanda L. Lewis[1,7] and Scott J. Hultgren[1*].

Affiliations:

[1]Department of Molecular Microbiology and Center for Women's Infectious Disease Research, Washington University School of Medicine, St. Louis, MO, USA.

[2]Department of Pathology and Immunology, Washington University School of Medicine, St. Louis, MO, USA.

[3]The Broad Institute of Massachusetts Institute of Technology and Harvard University, Cambridge, MA, USA.

[4]Internal Medicine, Division of Rheumatology, Washington University School of Medicine, St. Louis, MO, USA.

[5]Department of Genetics, Washington University School of Medicine, St. Louis, MO, USA.

[6]Departments of Urology and Genetics & Development, Columbia University, New York, NY, USA.

[7]Department of Obstetrics and Gynecology, Washington University School of Medicine, St. Louis, MO, USA.

*Correspondence to: hultgren@wusm.wustl.edu.

Supplementary Figures

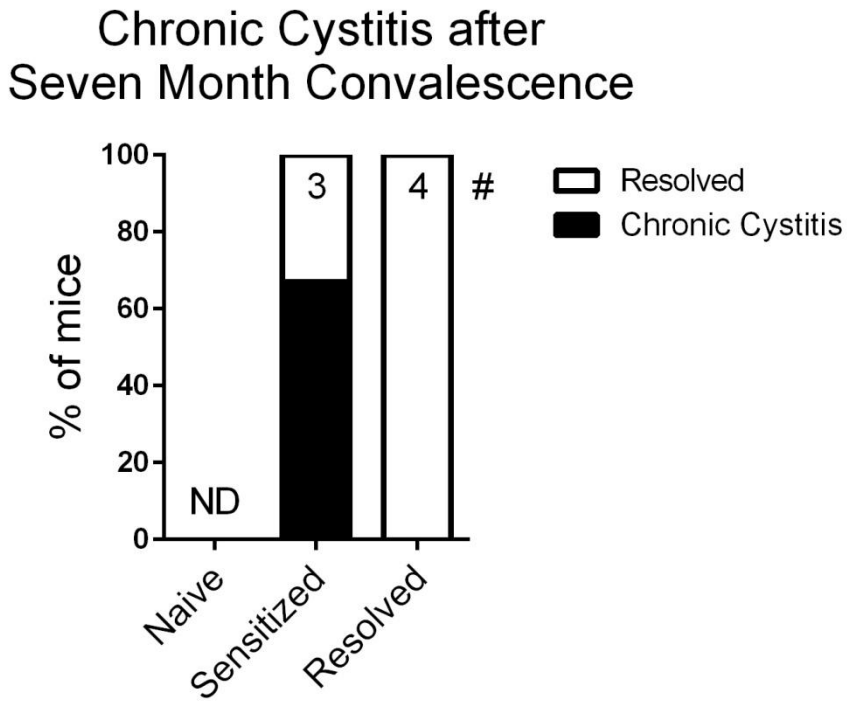

Supplementary Figure 1. Sensitized mice have long-lasting susceptibility to recurrent UTI. In this experiment the convalescent period in C3H/HeN mice was extended for seven months after the initiation of sterilizing antibiotic therapy. Shown is the incidence of chronic cystitis 28 dpi after challenge with 10^7 CFU UTI89. The # of mice per group is shown at the top of each bar; few mice were used because of the length of the experiments. ND, not determined. A 10^8 CFU dose was used in **Fig. 1b** because nulliparous C3H/HeN mice become resistant to UTI with age[1].

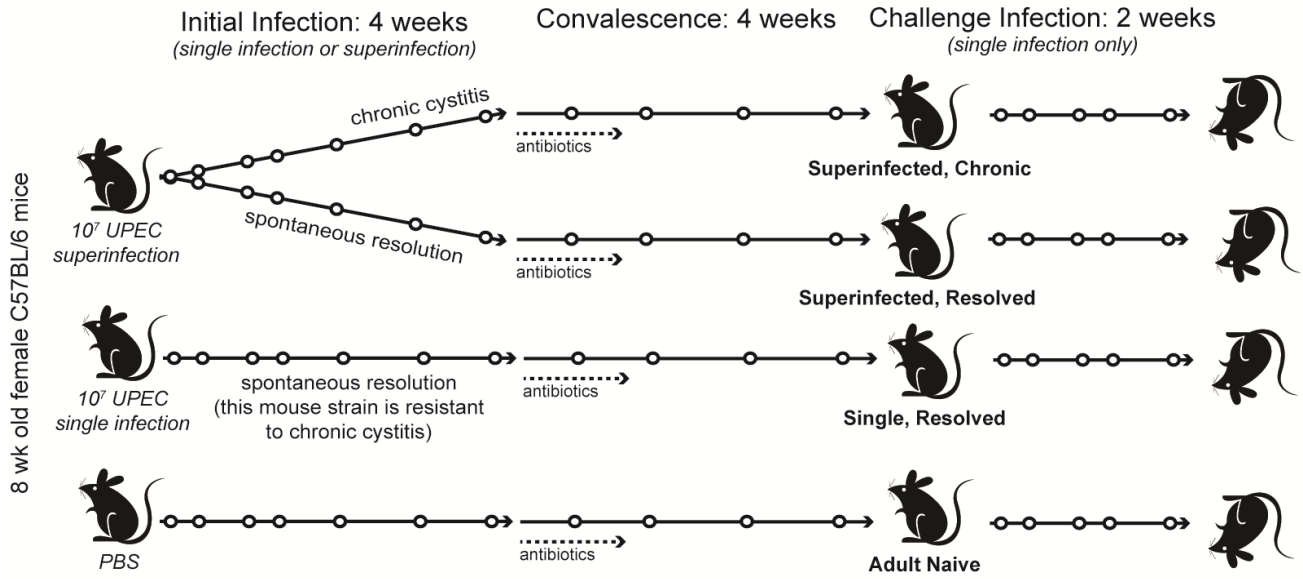

Supplementary Figure 2. Timeline of sensitization experiment in C57BL/6 mice shown in Fig. 1c. This inbred mouse strain is resistant to developing chronic cystitis upon infection with one dose of UPEC, but superinfection with two doses of 10^7 CFU UTI89 24 hours apart induces chronic cystitis (evidenced by persistent bacteriuria $>10^4$ CFU/ml for four weeks) in 30-35% of mice[2], denoted here as "Superinfected, Chronic." The 65-70% of mice that spontaneously resolve the superinfection are denoted here as "Superinfected, Resolved." As controls, mice initially were given one dose of UPEC ("Single, Resolved"), which all mice spontaneously resolved, or PBS ("Adult Naive"). Four weeks after the initial infection, all mice received antibiotics. Four weeks after the initiation of antibiotics, all mice were challenged with one dose of 10^7 CFU UTI89 and sacrificed after two weeks. Open circles indicate urine collection to monitor infection status.

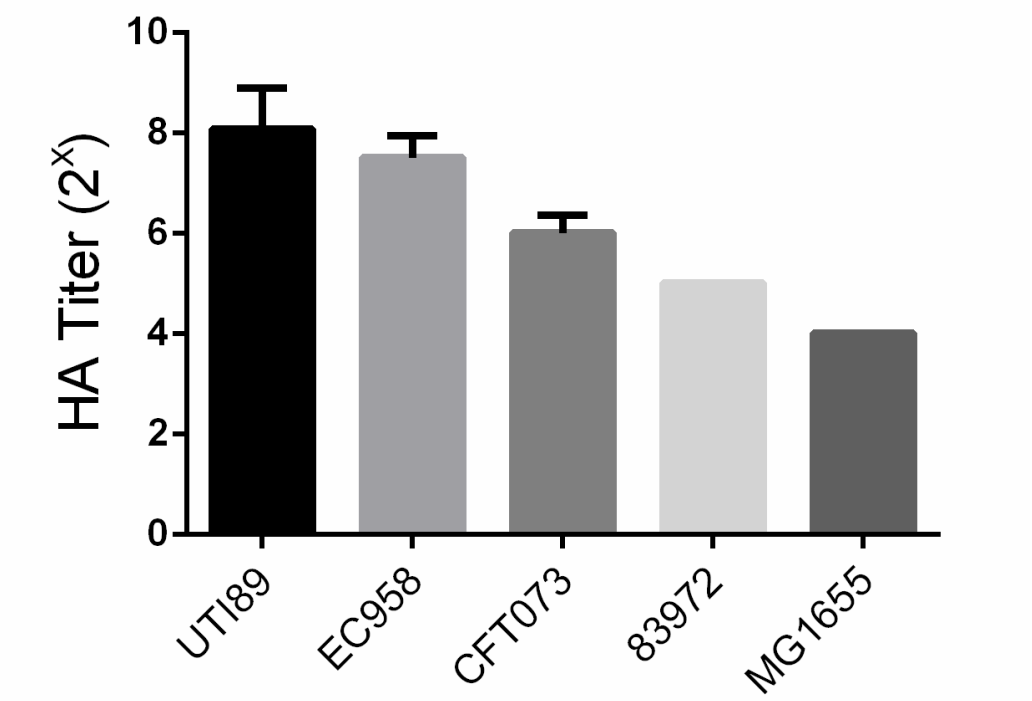

Supplementary Figure 3. Type 1 pilus expression in a panel of clinical *E. coli* isolates. Shown are the mean guinea pig red blood cell hemagglutination (HA) titers of indicated bacterial strains. Samples were tested in duplicate and N=2 replicate were performed; error bars indicate standard error of the mean.

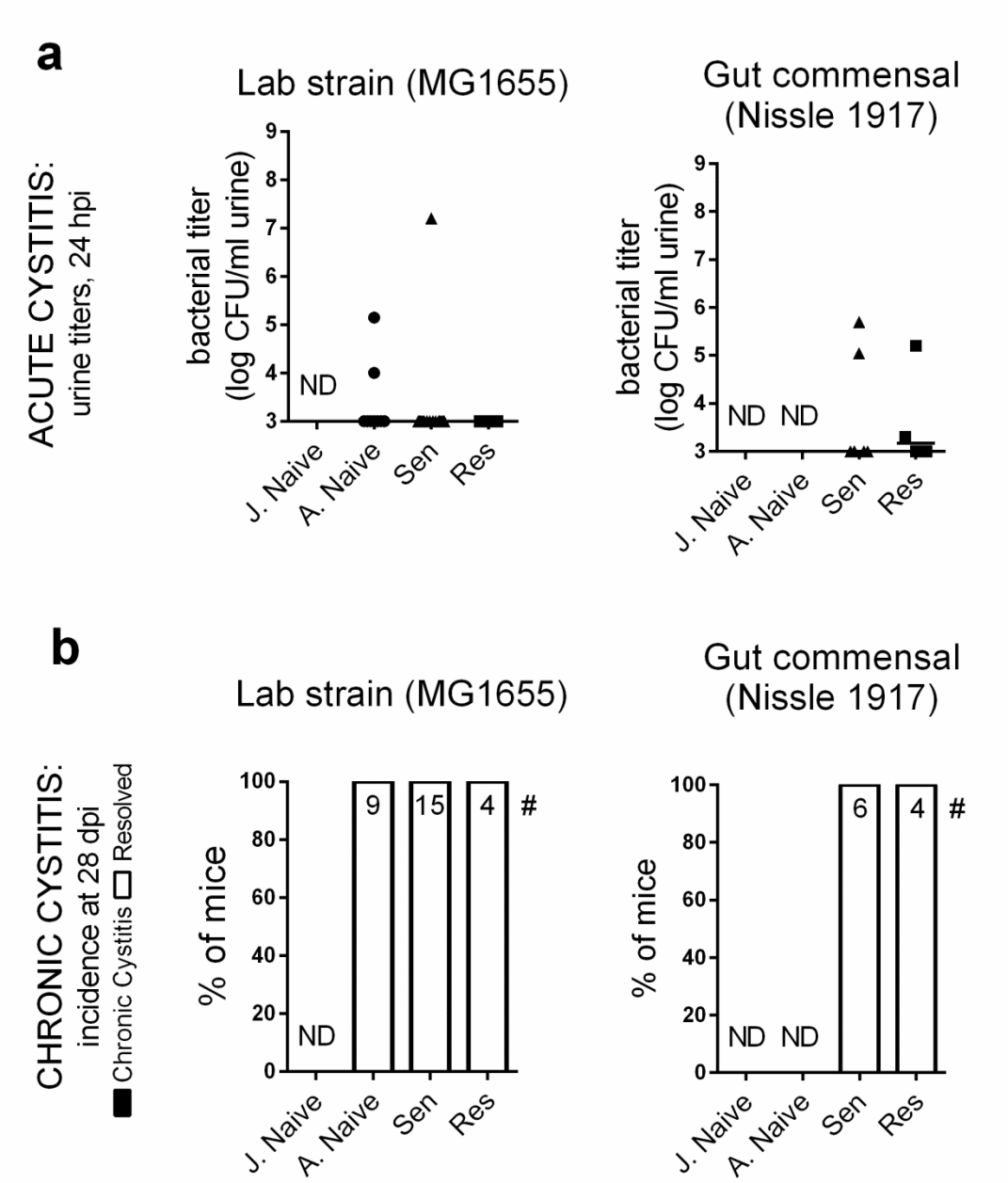

Supplementary Figure 4. Non-uropathogenic strains of *E. coli* were not pathogenic in Sensitized mice. Shown are (**a**) the urine bacterial burden at 24 hpi and (**b**) the incidence of chronic cystitis at 28 dpi after challenge infection with 10^7 CFU of the *E. coli* strains MG1655 and Nissle 1917. In panel **b**, the numbers at the top of each column represent the number of mice tested. ND, not determined. MG1655 was tested in N=2 replicates and Nissle 1917 was tested in N=1 replicate.

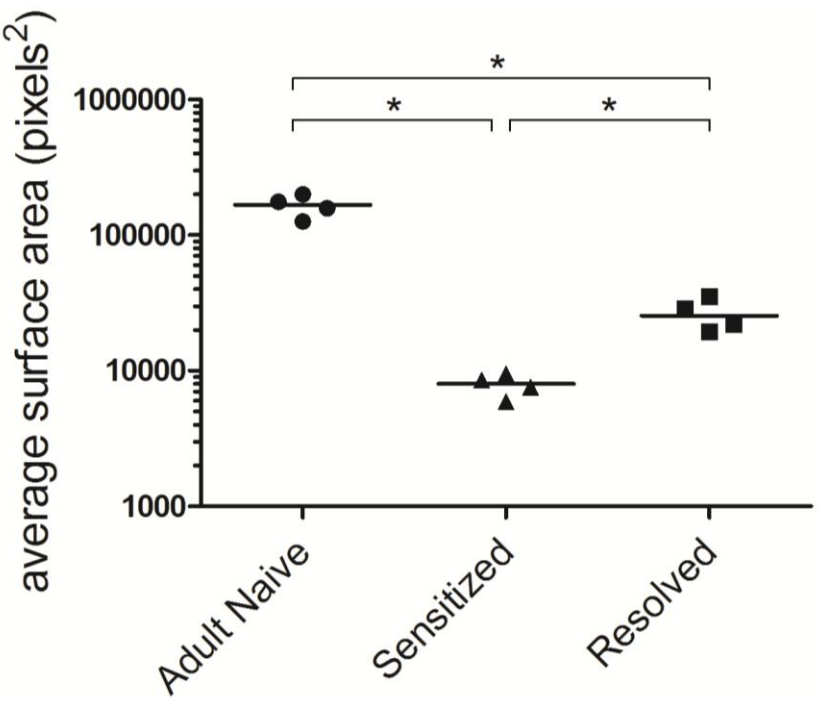

Supplementary Figure 5. Infection history impacts bladder cell size during convalescence. Shown is the average urothelial cell size (pixels^2) in convalescent mice sacrificed at one month after the initiation of ten days of oral trimethoprim-sulfamethoxazole antibiotics. Cell sizes were measured in ImageJ. Five 500x magnification scanning electron micrographs were taken per bladder half (total of ten images per mouse) and every cell that was completely contained within the image was measured. Data points represent the average of all measurements for a given mouse. * $P < 0.05$, Mann-Whitney U test.

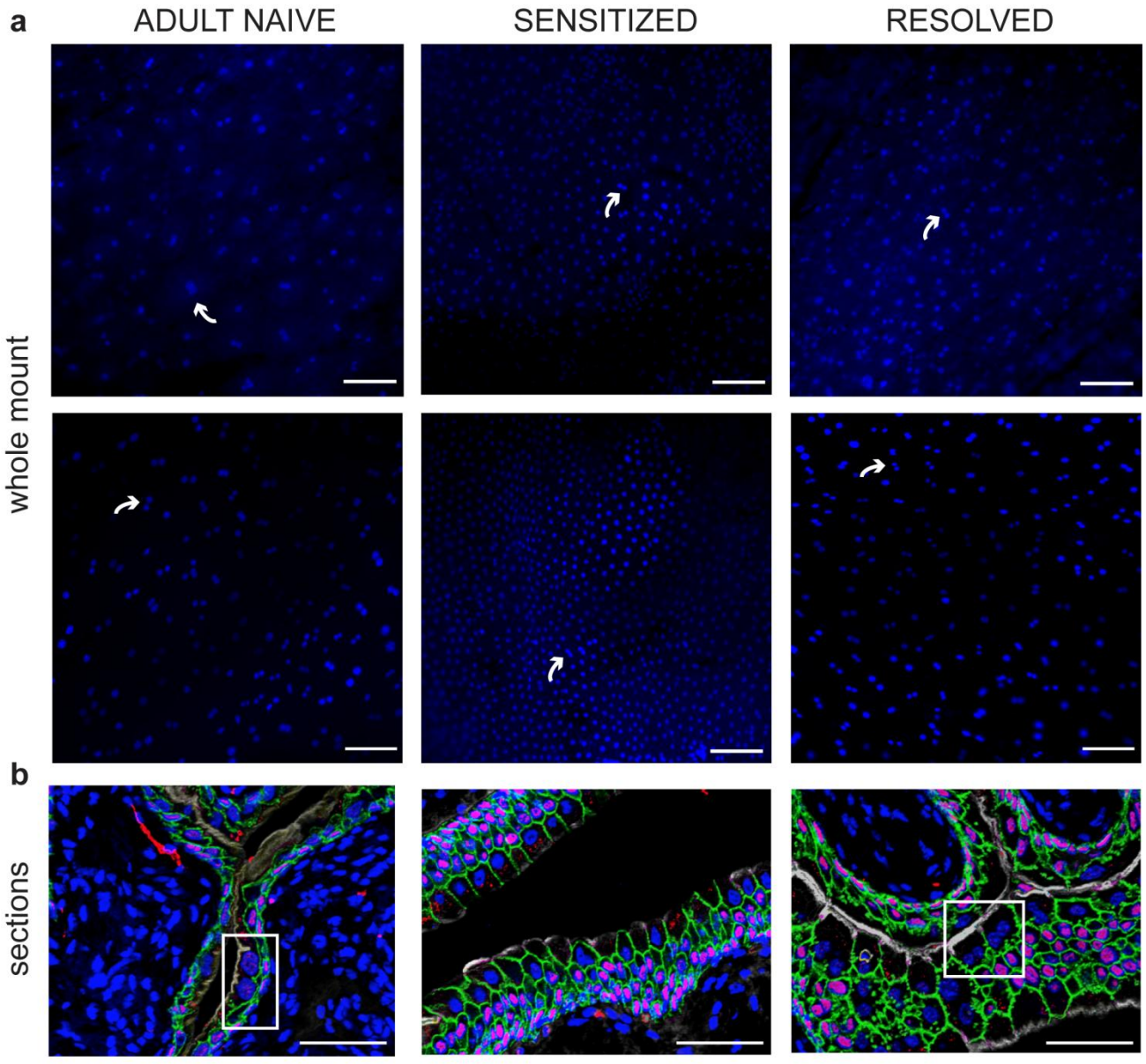
a
ADULT NAIVE
SENSITIZED
RESOLVED
whole mount
b
sections

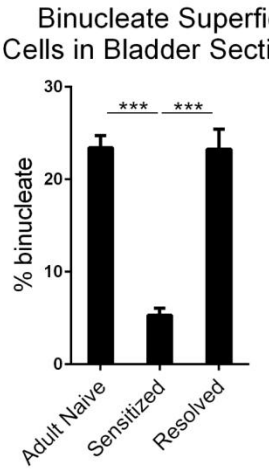
c
Binucleate Superficial Cells in Bladder Sections
% binucleate
30
20
10
0
***
***
Adult Naive
Sensitized
Resolved

Supplementary Figure 6. Few superficial cells in Sensitized mice were binucleate. (**a**) Representative images of DAPI-stained whole mounted bladders visualized by epifluorescence microscopy show more binucleate cells (arrows indicate examples) in Adult Naive and Resolved bladders than Sensitized bladders (N=1 replicate with n=3 bladders per group). Scale bars are 100 μm. Images in the first row are slightly overexposed to facilitate the visualization of individual cells. (**b**) Paraffin-embedded bladder sections were stained for keratin 20 (white), E-cadherin (green), Trp63 (red), and nuclei (blue) and visualized by fluorescence microscopy. Boxes denote examples of binucleate superficial cells (keratin 20+, Trp 63-, with a basolateral layer of E-cadherin). Scale bars are 50 μm. Representative images are shown from N=3 experiments with sections from n=3 Adult Naive and Resolved and n=6 Sensitized mice. (**c**) Nuclei were enumerated in all superficial cells ($TRP63^-$, keratin 5^-, uroplakin $IIIa^+$, keratin 20^+ [weak/patchy staining observed in Sensitized mice], with a basolateral band of E-cadherin) in stained bladder sections from the experiment in panel **b**, and the percentage of binucleate cells was calculated. Only 5.3% of luminal cells in Sensitized mice were binucleate, compared to 23.4% and 23.3% of superficial cells in Adult Naive and Resolved mice, respectively. Shown is the average percentage of binucleate superficial cells among all bladders from a given group of mice; error bars represent standard error of the means; *** $P < 0.001$, Fisher's exact test. Note the smaller superficial cell size in Sensitized and Resolved mice relative to Adult Naive mice.

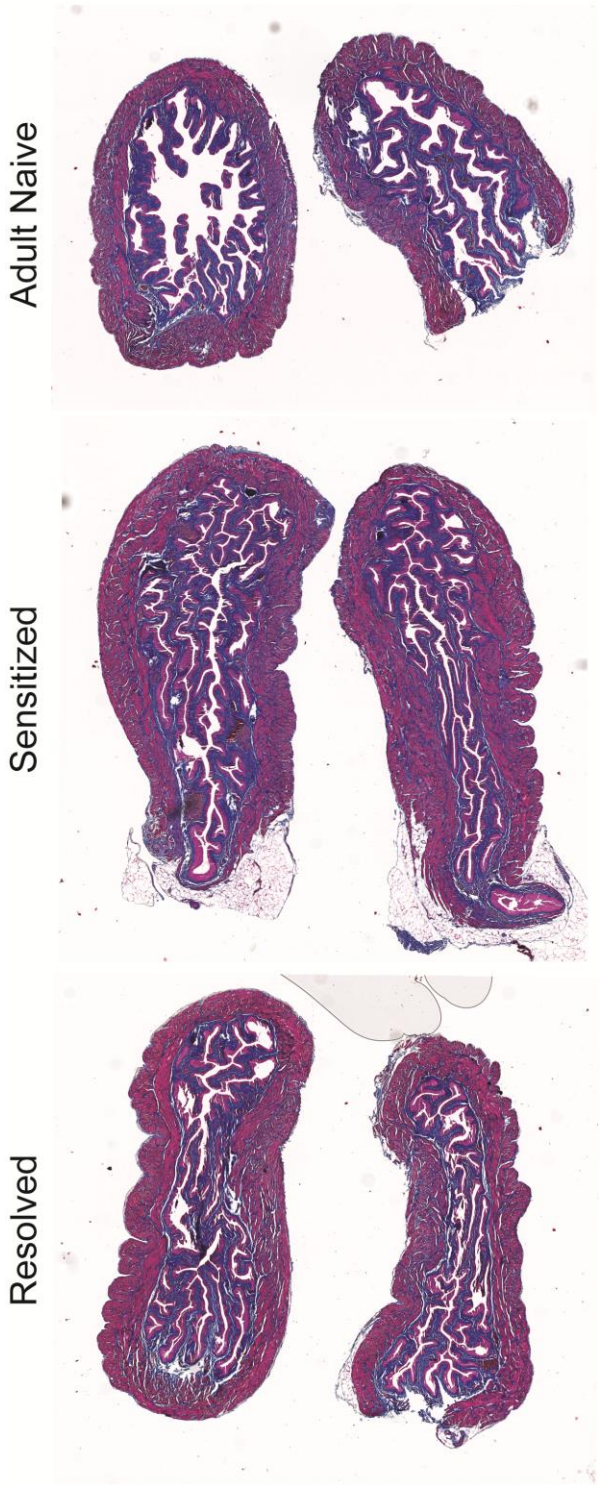

Supplementary Figure 7. Masson's trichrome staining for collagen deposition did not reveal fibrosis in convalescent mice. Shown are representative brightfield images of whole bladder sections at 20x magnification from n=3-7 mice per group (N=2). Keratin and muscle stain purple and collagen stains blue by this method[3]; in a blinded analysis, there was no difference in collagen deposition among the mice.

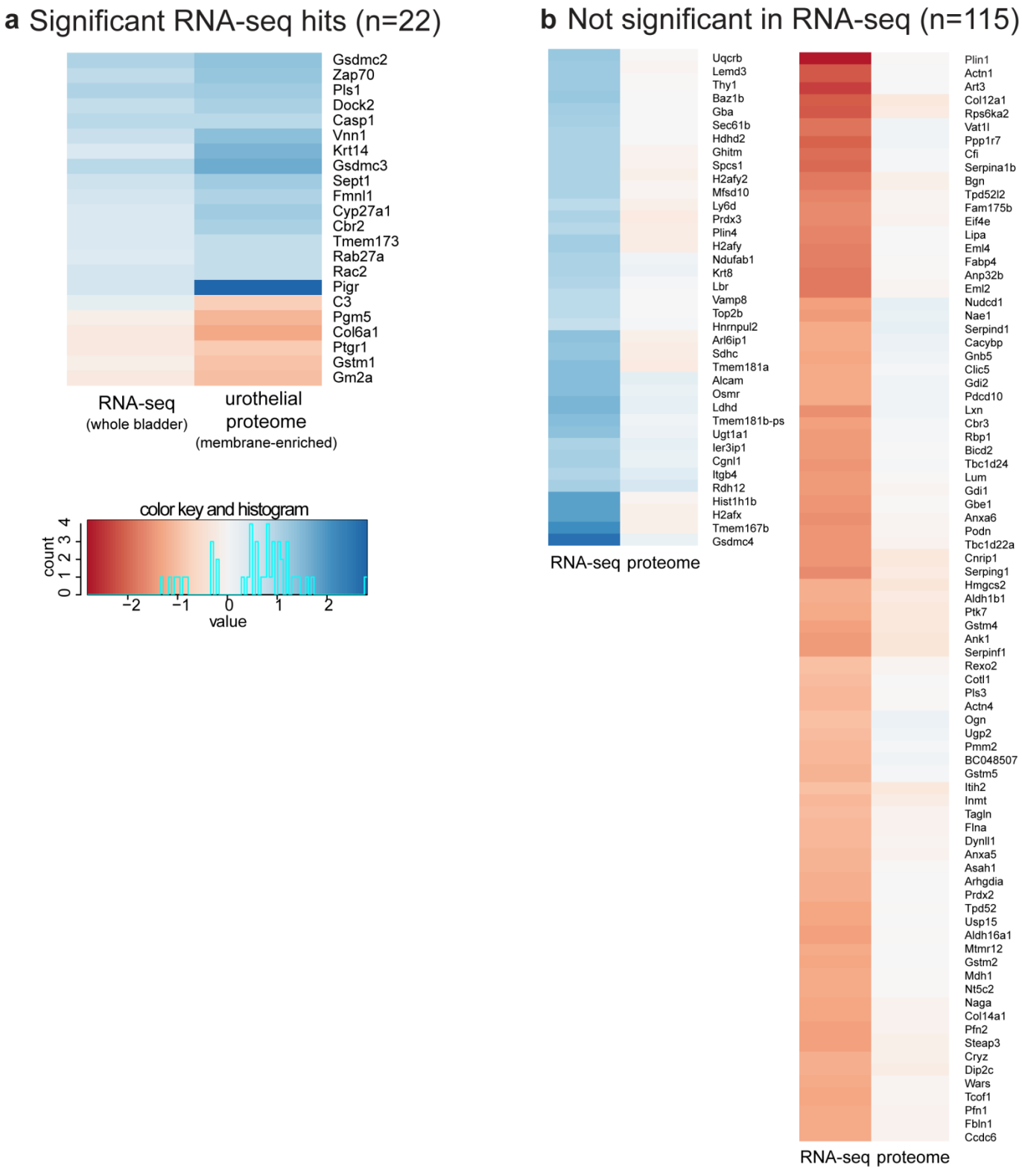
a Significant RNA-seq hits (n=22)
Gsdmc2
Zap70
Pls1
Dock2
Casp1
Vnn1
Krt14
Gsdmc3
Sept1
Fmnl1
Cyp27a1
Cbr2
Tmem173
Rab27a
Rac2
Pigr
C3
Pgm5
Col6a1
Ptgr1
Gstm1
Gm2a
RNA-seq
(whole bladder)
urothelial
proteome
(membrane-enriched)
color key and histogram
count
0 1 2 3 4
−2 −1 0 1 2
value
b Not significant in RNA-seq (n=115)
Uqcrb
Lemd3
Thy1
Baz1b
Gba
Sec61b
Hdhd2
Ghitm
Spcs1
H2afy2
Mfsd10
Ly6d
Prdx3
Plin4
H2afy
Ndufab1
Krt8
Lbr
Vamp8
Top2b
Hnrnpul2
Arl6ip1
Sdhc
Tmem181a
Alcam
Osmr
Ldhd
Tmem181b-ps
Ugt1a1
Ier3ip1
Cgnl1
Itgb4
Rdh12
Hist1h1b
H2afx
Tmem167b
Gsdmc4
RNA-seq proteome
Plin1
Actn1
Art3
Col12a1
Rps6ka2
Vat1l
Ppp1r7
Cfi
Serpina1b
Bgn
Tpd52l2
Fam175b
Eif4e
Lipa
Eml4
Fabp4
Anp32b
Eml2
Nudcd1
Nae1
Serpind1
Cacybp
Gnb5
Clic5
Gdi2
Pdcd10
Lxn
Cbr3
Rbp1
Bicd2
Tbc1d24
Lum
Gdi1
Gbe1
Anxa6
Podn
Tbc1d22a
Cnrip1
Serping1
Hmgcs2
Aldh1b1
Ptk7
Gstm4
Ank1
Serpinf1
Rexo2
Cotl1
Pls3
Actn4
Ogn
Ugp2
Pmm2
BC048507
Gstm5
Itih2
Inmt
Tagln
Flna
Dynll1
Anxa5
Asah1
Arhgdia
Prdx2
Tpd52
Usp15
Aldh16a1
Mtmr12
Gstm2
Mdh1
Nt5c2
Naga
Col14a1
Pfn2
Steap3
Cryz
Dip2c
Wars
Tcof1
Pfn1
Fbln1
Ccdc6
RNA-seq proteome

Supplementary Figure 8. Whole bladder RNA-seq findings are in concordance with the previously published urothelial membrane proteome. Of the 156 most significantly enriched or depleted proteins in the Sensitized urothelial proteome[4] ($P_{adjusted} < 0.01$), 22 were also significantly differentially expressed by RNA-seq ($P_{adjusted} < 0.05$) (**a**) and the majority were changed in the same direction (**b**), demonstrating that urothelial remodeling is at least partially controlled at the transcriptional level. The 22 genes were among the most enriched/depleted proteins from the proteomic analysis, and include cytoskeleton-associated proteins like keratin 14 (*Krt14*), septin-1 (*Sept1*) and formin-like protein-1 (*Fmnl1*); extracellular matrix-associated proteins like collagen (*Col6a1*); cell death-associated proteins such as caspase 1 and gasdermins Gsdmc2 and Gsdmc3; and the polymeric immunoglobulin receptor Pigr. See **Supplementary Table 2** for *P* values and fold changes. Proteomics data are from N=1 experiment with n=3 mice per group[4] and RNA-seq data are from N=1 experiment with n=7 Sensitized and n=6 Resolved mice.

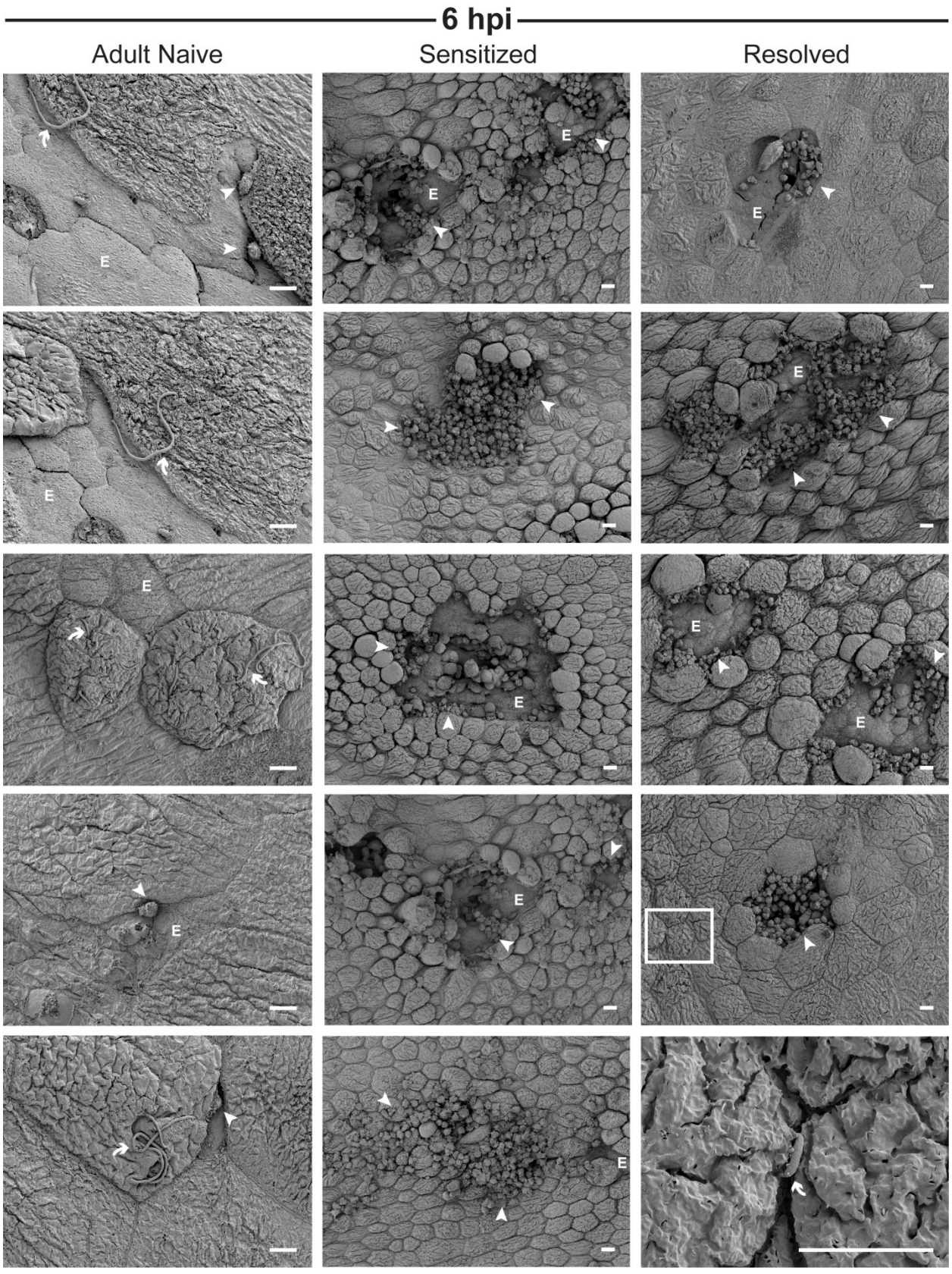
6 hpi
Adult Naive
Sensitized
Resolved
E

Supplementary Figure 9. UTI history impacted host responses at 6 hpi. Additional representative scanning electron micrographs of the luminal surface of bladders at 6 hpi with 10^8 CFU UTI89 are shown. N=2 experiments with n=3-4 bladders per group. Curved arrows show bacteria; arrowheads show neutrophils; "E" denotes regions of exfoliation. All scale bars are 10 μm; Adult Naive images are shown at a higher magnification (1000x) than Sensitized and Resolved mice (500x) to facilitate the visualization of bacterial filaments. One rod-shaped bacterium (denoted by a box) was detected in a Resolved bladder and is shown at 5000x magnification directly underneath the lower magnification image.

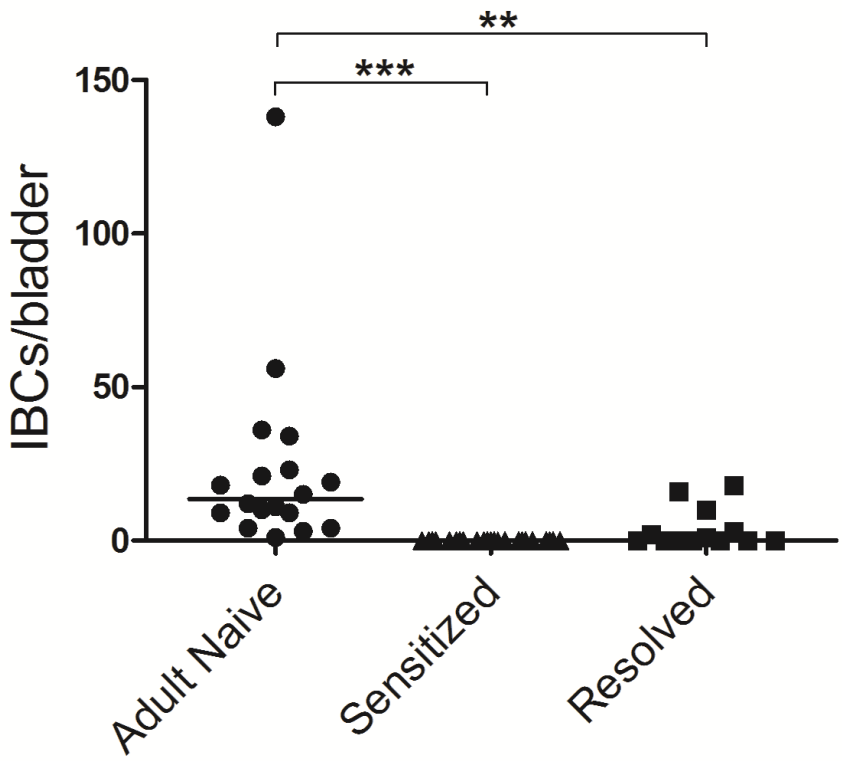

Supplementary Figure 10. Intracellular bacterial communities (IBCs) were not detected in Sensitized mice by a β-galactosidase activity assay. Mice were challenged with 10^7 CFU UTI89 and sacrificed at 6 hpi. After X-gal staining for β-galactosidase activity, IBCs were visualized using a dissection microscope. ** $P < 0.01$, *** $P < 0.001$, Mann-Whitney *U* test. Data are from N=2 experiments performed in parallel by two separate investigators. Data points represent actual values for each individual mouse.

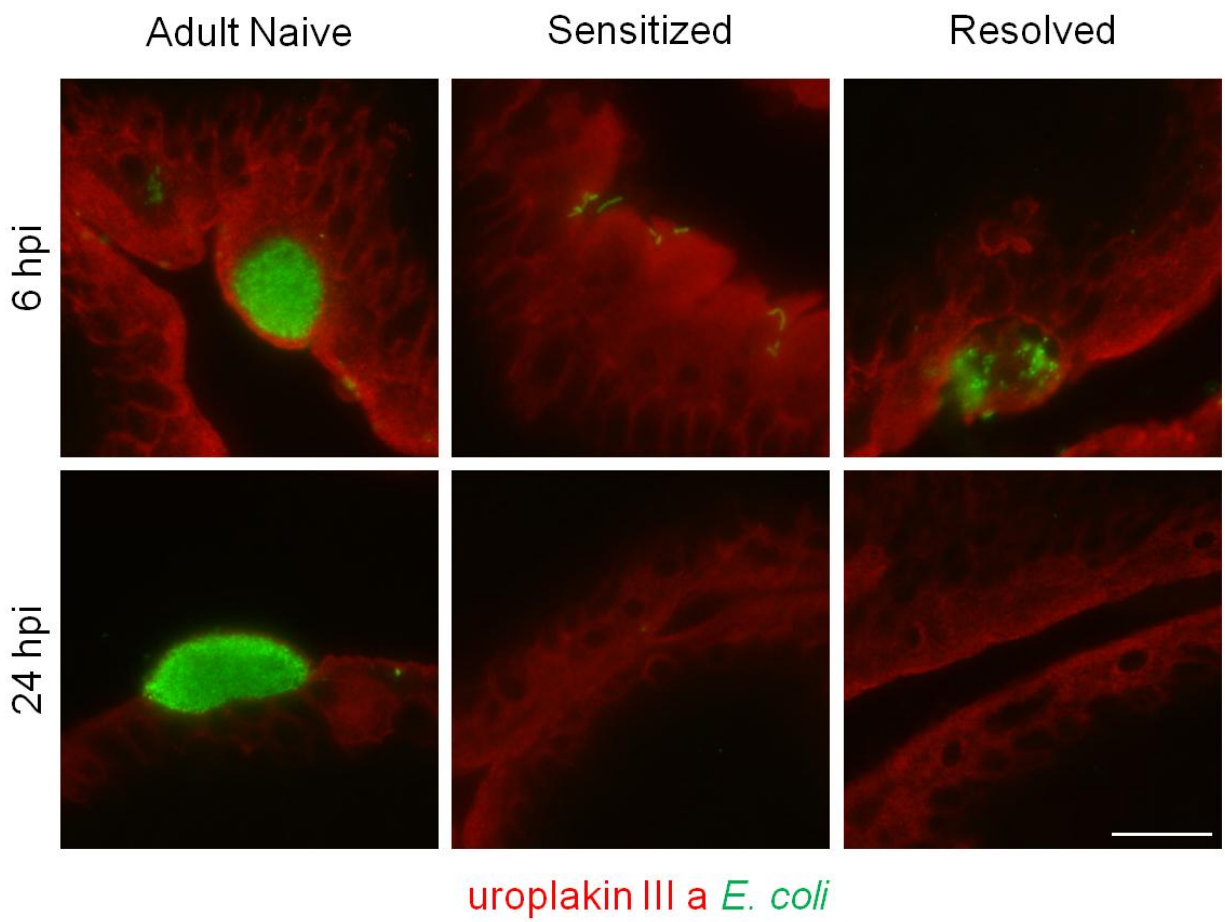

Supplementary Figure 11. Intracellular bacterial communities (IBCs) were not detected in Sensitized mice by immunofluorescence. Mice were challenged with 10^8 CFU UTI89 and bladders were fixed in methacarn at 6 or 24 hpi, embedded in paraffin and sectioned. Deparaffinized bladder sections were stained for *E. coli* (green) and uroplakin IIIa (red) and visualized by epifluorescence. Shown are representative images at the same magnification from n=3-5 bladders per mouse per time point from N=1 experiment. Scale bar is 200 µm.

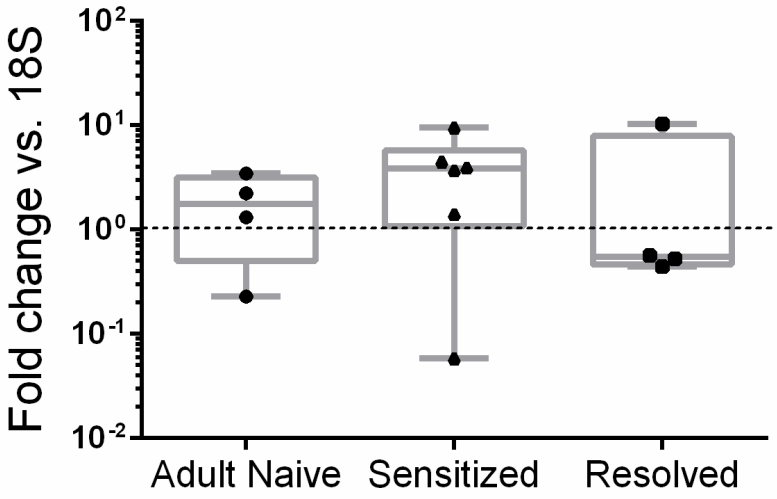

Supplementary Figure 12. **During convalescence, UTI history did not influence expression of the COX-2 gene, *Ptgs2*.** qRT-PCR was used to assess bladder *Ptgs2* expression relative to 18S expression in mock-infected Adult Naive, Sensitized and Resolved bladders. Data points represent actual values for each individual mouse, bars indicate median values and whiskers are min to max values.

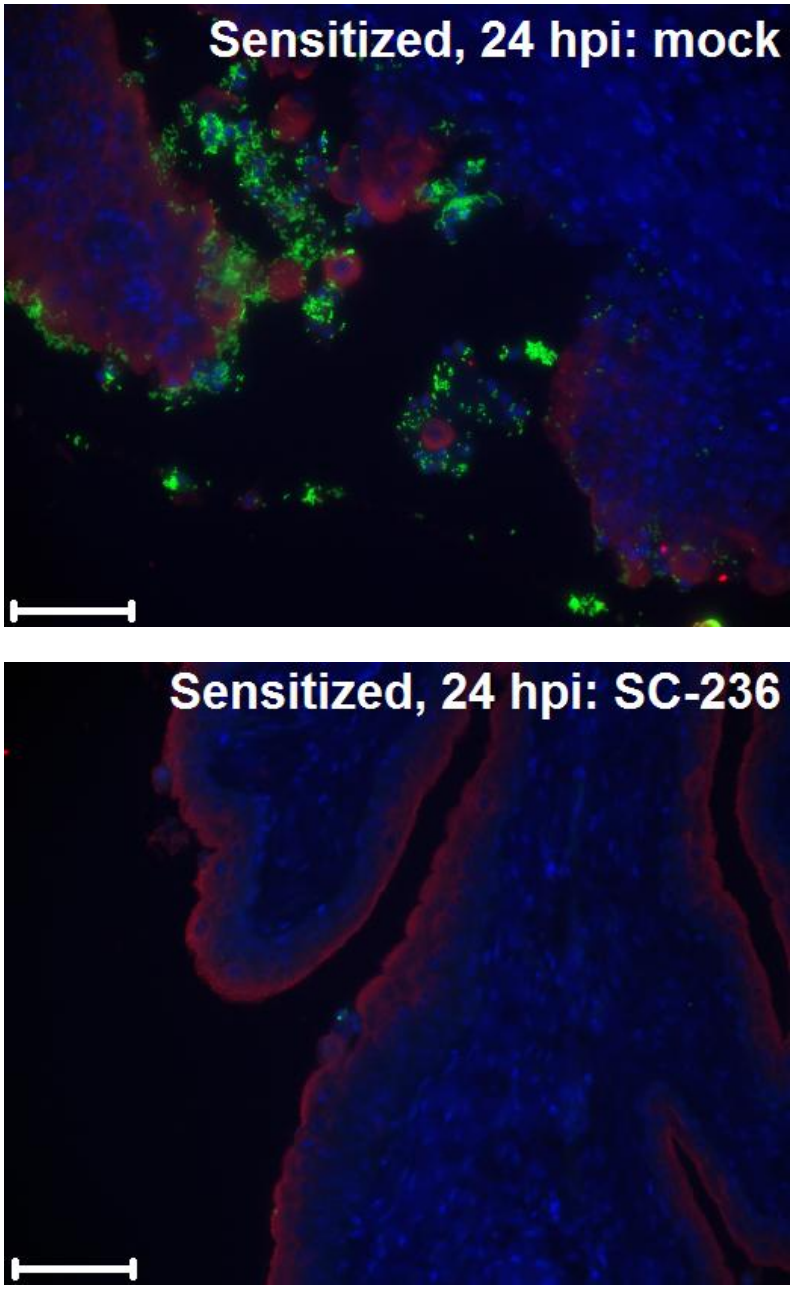

Supplementary Figure 13. **Inhibition of cyclooxygenase-2 (COX-2) prior to challenge prevented mucosal wounding in Sensitized mice.** Mice were pre-treated with buffer (top image) or the COX-2 inhibitor SC-236 (bottom image) and then infected for 24 hpi with 10^7 CFU UTI89. Most mice were used to assess bladder colonization as shown in **Fig. 4f**; bladders from n=3 inhibitor-treated and n=3 SC-236-treated Sensitized mice from N=1 experiment were preserved for microscopy experiments. Deparaffinized bladder sections were stained for *E. coli* (green), uroplakin III (red) and DNA (blue) and visualized by epifluorescence. Bacterial colonization and mucosal wounding was detected in 1 of 3 buffer-treated bladders (representative image shown) and 0 of 3 inhibitor-treated bladders. Scale bars are 500 μm.

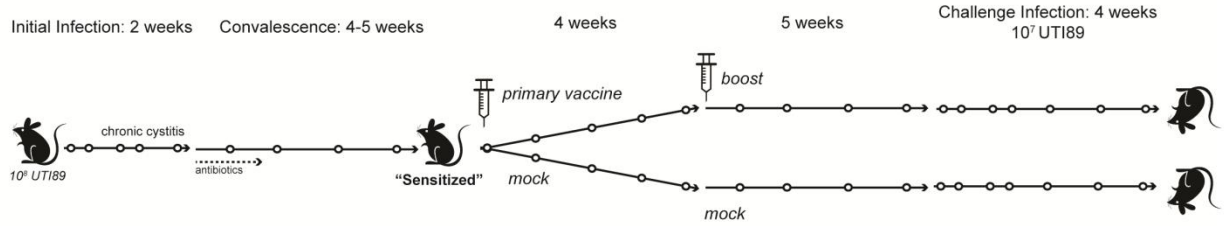

Supplementary Figure 14. Time course of FimH vaccination experiments in Sensitized mice. The initial infection with 10^8 CFU UTI89 was shortened to two weeks, which is sufficient to cause sensitization[5]. After antibiotic-induced convalescence, mice were vaccinated subcutaneously with 15 μg FimCH (FimH adhesin in complex with its chaperone protein FimC) emulsified 1:1 with Complete Freund's Adjuvant (CFA) for the primary vaccine or Incomplete Freund's Adjuvant (IFA) for the boost. For negative controls, mice received buffer and CFA/IFA, or 15 μg of the FimC chaperone protein alone and CFA/IFA. FimC was previously shown not to be protective against UTI[6]. The buffer and FimC groups are combined and presented as "mock" in **Figure 4e** and **4f** as they were statistically indistinguishable. Five weeks after boosting, mice were challenged with 10^7 CFU UTI89. Open circles indicate urine collection to monitor infection status.

Supplementary Tables

Supplementary Table 1: Gene list from whole-bladder RNA-seq experiment, in which gene expression was compared between Sensitized and Resolved mice during convalescence (four weeks after the initiation of antibiotics). Significantly differentially expressed genes are shown in green. Significance was determined using a Wald test and adjusted for multiple comparisons using the Benjamini-Hochberg false-discovery rate correction, with $P_{adjusted} < 0.05$ deemed significantly differentially expressed. RNA-seq data has been deposited at NCBI under the BioProject ID number PRJNA327807.

Supplementary Table 2: The fold changes in gene expression from whole-bladder RNA-seq, compared to the fold enrichment/depletion of the most significantly enriched/depleted proteins ($P_{adjusted} < 0.01$) from a previously published analysis of the urothelial proteome enriched for membrane-associated glycoproteins[4] (grey columns). Genes/proteins that were significant in both analyses are shown in green. N/A, not applicable (due to all samples in a group having no counts).

Supplementary Table 3: Pathway analysis showing the canonical pathways enriched in the differentially expressed genes in the RNA-seq experiment. See Legend in the second tab.

Supplementary Table 4: Broad meta-pathways assembled by Ingenuity IPA from the specific enriched pathways given in **Supplementary Table 3**. In the histogram in **Fig. 2e**, the smallest *P* value from the range of *P* values in column B is reported.

Supplementary References

1 Kline, K. A., Schwartz, D. J., Gilbert, N. M. & Lewis, A. L. Impact of host age and parity on susceptibility to severe urinary tract infection in a murine model. *PLoS One* **9**, e97798, doi:10.1371/journal.pone.0097798 (2014).

2 Schwartz, D. J., Conover, M. S., Hannan, T. J. & Hultgren, S. J. Uropathogenic Escherichia coli superinfection enhances the severity of mouse bladder infection. *PLoS Pathog* **11**, e1004599, doi:10.1371/journal.ppat.1004599 (2015).

3 Metcalfe, P. D. *et al.* Bladder outlet obstruction: progression from inflammation to fibrosis. *BJU international* **106**, 1686-1694, doi:10.1111/j.1464-410X.2010.09445.x (2010).

4 Hannan, T. J. *et al.* Inhibition of Cyclooxygenase-2 Prevents Chronic and Recurrent Cystitis. *EBioMedicine* **1**, 46-57, doi:10.1016/j.ebiom.2014.10.011 (2014).

5 Hannan, T. J., Mysorekar, I. U., Hung, C. S., Isaacson-Schmid, M. L. & Hultgren, S. J. Early severe inflammatory responses to uropathogenic E. coli predispose to chronic and recurrent urinary tract infection. *PLoS Pathog* **6**, e1001042, doi:10.1371/journal.ppat.1001042 (2010).

6 Langermann, S. *et al.* Prevention of mucosal Escherichia coli infection by FimH-adhesin-based systemic vaccination. *Science* **276**, 607-611 (1997).